

THE ETA-II INDUCTION LINAC AS A HIGH-AVERAGE-POWER FEL DRIVER *

W.E. NEXSEN, D.P. ATKINSON, D.M. BARRETT, Y.-J. CHEN, J.C. CLARK, L.V. GRIFFITH,
H.C. KIRBIE, M.A. NEWTON, A.C. PAUL, S. SAMPAYAN, A.L. THROOP and W.C. TURNER

Lawrence Livermore National Laboratory, University of California, P.O. Box 808, Livermore, CA 94550, USA

The Experimental Test Accelerator II (ETA-II) is the first induction linac designed specifically to FEL requirements. It is primarily intended to demonstrate induction accelerator technology for high-average-power, high-brightness electron beams, and will be used to drive a 140 and 250 GHz microwave FEL for plasma heating experiments in the Microwave Tokamak Experiment (MTX) at LLNL. Its features include high-vacuum design which allows the use of an intrinsically bright dispenser cathode, induction cells designed to minimize BBU growth rate, and careful attention to magnetic alignment to minimize radial sweep due to beam corkscrew. The use of magnetic switches allows high-average-power operation. At present ETA-II is being used to drive 140 GHz plasma heating experiments. These experiments require nominal beam parameters of 6 MeV energy, 2 kA current, 20 ns pulse width and a brightness of $1 \times 10^8 \text{ A}/(\text{m rad})^2$ at the wiggler with a pulse repetition frequency (prf) of 0.5 Hz. Future 250 GHz experiments require beam parameters of 10 MeV energy, 3 kA current, 50 ns pulse width and a brightness of $1 \times 10^8 \text{ A}/(\text{m rad})^2$ with a 5 kHz prf for 0.5 s. In this paper we discuss the present status of ETA-II parameters and the phased development program necessary to satisfy these future requirements.

1. Introduction

The Experimental Test Accelerator II (ETA-II) program's principle goal is to develop and demonstrate the induction linac technology necessary for driving FELs at high average power (HAP). We will use ETA-II to drive 140 GHz and 250 GHz microwave FELs at an average power of 1–2 MW. The FEL output will be used for plasma heating experiments on the LLNL Microwave Tokamak Experiment (MTX). The program includes not only the operation of the accelerator itself

but also of test stands for studying cathode brightness and poisoning, ferrite response, multicable cell block feeds, and the operation of magnetic switches at high repetition frequency (prf). An extensive modeling and computational effort supports the experiments.

ETA-II is the first induction linac designed specifically to FEL requirements. As presently configured it can supply a 3 kA, 6 MeV, 70 ns full-width-at-half-maximum pulse at 1 Hz; this satisfies the requirements for the initial 140 GHz experiments. Future 250 GHz HAP experiments require increasing the beam energy to 10 MeV, with $\pm 1\%$ energy regulation for 50 ns and a 5 kHz prf for 0.5 s. In the following sections we describe some of ETA-II's unique features and discuss the development program underway to satisfy the ultimate goal of high average power. The performance goals of the ETA-II program are listed in table 1.

* Work performed under the auspices of the US Department of Energy by the Lawrence Livermore National Laboratory under W-7405-ENG-48. ETA-II accelerator development is part of the SDIO/SDC induction-linac free electron laser Science and Technology Program.

Table 1
Goals and current status of ETA-II parameters

Parameter	Goal	Current status
Brightness [$\text{A}/\text{m}^2 \text{ rad}^2$]	$> 2 \times 10^9$	5×10^9
Current [kA]	3	> 3
Beam energy [MeV]	6	6
	10	–
Energy sweep (head to tail)	$\pm 1\%$, 50 ns	$\pm 1\%$, 10 ns
Energy stability (pulse to pulse)	$\pm 0.1\%$	–
Flux line alignment [μm]	± 100	–
Centroid displacement [mm]	< 1 , 50 ns	10, 10 ns
Repetition rate [kHz]	5	5 (test stand)
Duration [s]	0.5	0.08 (test stand)

2. ETA-II design features

2.1. Injector design

Power supply limitations necessitated an injector design which would supply a 3 kA beam current from a space-charge-limited cathode for an anode-cathode (A-K) voltage difference of 1 MV. The DPC code [1] was used to design a diode configuration with a 12.7 cm diameter cathode (radius of curvature = 36.5 cm) and an A-K gap distance of 7.6 cm (fig. 1a). For the electron source, which must satisfy stringent requirements for current density, uniformity, repetition rate, heat load and brightness, we chose an osmium-coated "M"-type dispenser cathode which is capable of pulse current densities greater than 50 A/cm² and has an intrinsic brightness exceeding 1 × 10¹⁰ A/(m rad)² [2]. This design is now used on ETA-II. The experimental *I-V* data obtained from this injector agrees well with the predictions of the DPC code (fig. 1b).

2.2. Induction cell design

The accelerator cell design is shown in fig. 2a. It is a compromise between conflicting requirements for minimizing the growth rate for the beam breakup (BBU) instability and maximizing the voltage gradient while avoiding high-voltage breakdown of the vacuum gaps or surface breakdown of the insulators. The BBU exponential growth scales as Nw/a^2 where N is the number of gaps through which the beam passes, w is the gap width and a is the beam-pipe radius [3]. For a given final beam energy, decreasing N raises the voltage per gap while decreasing the gap width increases the electric

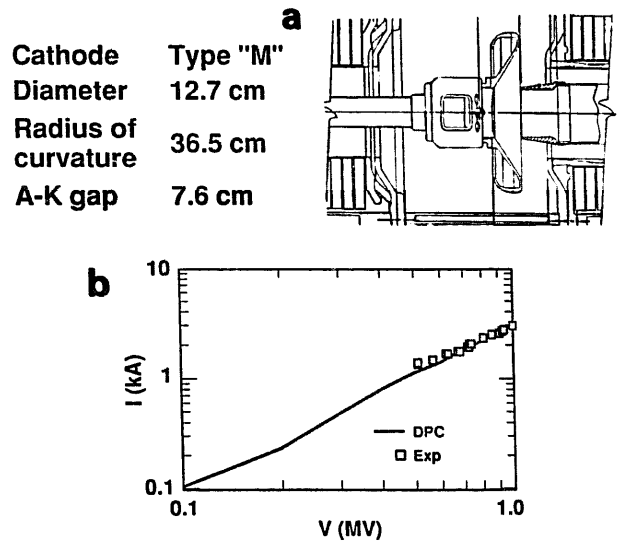


Fig. 1. (a) ETA-II 3 kA, 1 MeV diode injector design. (b) Experimental *I-V* data compared with DPC predictions.

field. For a constant volt-second product the volume of ferrite increases linearly with radius, soon reaching a practical upper limit. The ETA-II cell has a pipe radius of 13.2 cm and a gap width of 0.75 cm. ETA-II is presently configured with six ten-cell blocks ($N = 60$). (There are plans to increase N to 80 in the future.) To reduce the Q of the cavity formed by the gap, whose beam-excited asymmetric fields drive the BBU, the alumina insulator is designed so that radially propagating waves strike it at the Brewster angle and are almost totally transmitted through it into the cell. Once through the insulator they are reflected into the ferrite region where they are absorbed almost completely [4].

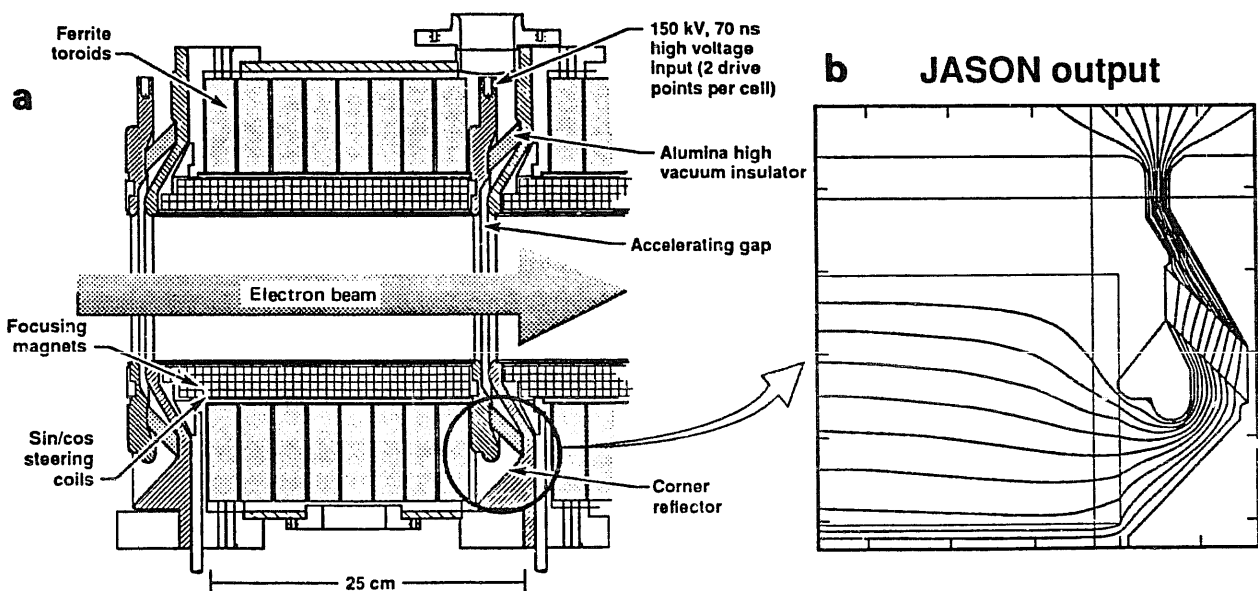


Fig. 2. (a) ETA-II accelerator induction cell design. (b) JASON output showing equipotentials in the accelerator gap and insulator regions.

The insulator and gap geometry are designed to minimize the maximum field stress on them. The JASON code [5] was used to calculate equipotential surfaces in test designs. The equipotentials for the final cell design are shown in fig. 2b. At 150 kV per gap the maximum field stress in the gap is 200 kV/cm while along the vacuum surface of the insulator the field is uniform and less than 50 kV/cm.

Another feature of the cell design is the attempt to improve the ferrite loading characteristic by having it resemble a ferrite-loaded coaxial transmission line driven axially from one end. The superiority of this approach over previous designs has been demonstrated by measurements reported in ref. [6].

2.3. Magnetic switches

Since the individual linac pulse widths are of the order of 50 ns, the goal of high average power can only be reached practically by high-repetition-rate operation (5 kHz prf for ETA-II). It is not possible to reach this prf with spark gap switching which was used in the older accelerators; consequently four magnetic pulse compressors (Mag-1Ds), each capable of > 5 GW instantaneous and > 1 MW average power [4], are used for the switching of the pulsed-power units (PPUs). One PPU feeds the injector while the others each feed twenty cells.

3. ETA-II operation

ETA-II and its associated test stands are involved in a phased development program whose final objective is

to demonstrate the ability of induction linacs to drive FELs at high average power. As shown in table 1, the ability to satisfy many of the parametric requirements necessary for meeting this objective has been demonstrated either on ETA-II or a test stand. In the process we have solved some serious problems and, for the present, have been able to live with others. Of the latter category we have solutions waiting to be implemented for almost all.

3.1. Injector vacuum requirements

So far as we are aware we are the first to use the type-"M" cathode, which is normally run in the hard vacuum of a sealed-off tube, in an accelerator vacuum environment. In early operation of ETA-II we were troubled by poisoning of the cathode emission. This was caused by the background pressure of Freon 113 which was used as coolant and insulating liquid in the induction cells and which had diffused through the Buna O-rings into the high-vacuum chamber. Test-stand poisoning studies [7] showed that the cathode emission was very sensitive to the partial pressure of Freon 113 in the background gas while it was less sensitive to a substitute liquid, Fluorinert (FC75) (fig. 3). In addition it was determined that Viton O-rings were essentially impervious to the Fluorinert. Substitution of Fluorinert (FC75) and Viton O-rings in the ETA-II induction cells resulted in injector base pressures (with the cathode hot) in the low 10^{-8} Torr range with residual gases being mainly water vapor and CO. These two substitutions eliminated the cathode poisoning.

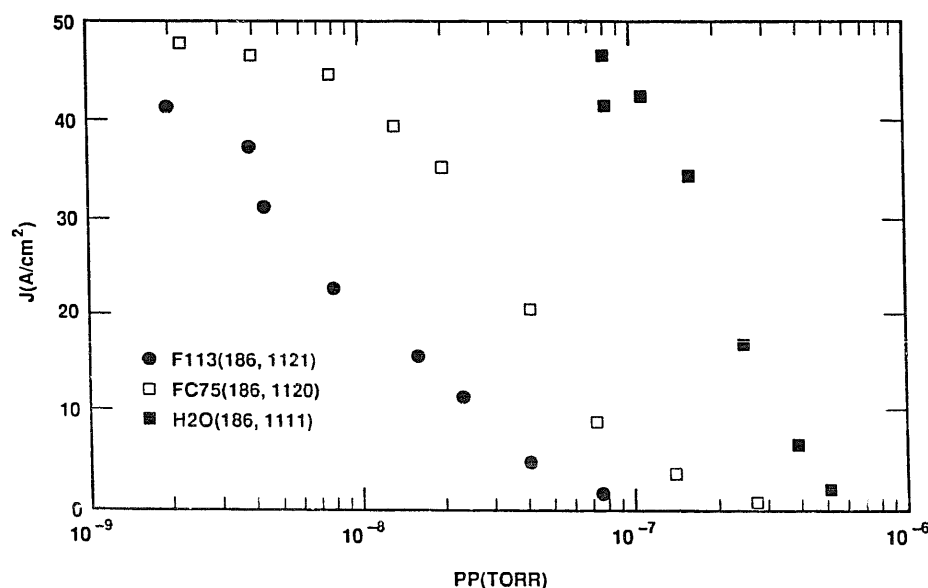


Fig. 3. "M"-type dispenser cathode emission current density as a function of the partial pressure of Fluorinert (FC75), Freon 113 and water vapor ($E = 186$ kV/cm, $T = 1120^\circ\text{C}$ (brightness)).

3.2. Cell operation

With the new cell design we did not expect to be bothered by a BBU in a machine as short as ETA-II and, indeed, no evidence of the BBU has been seen at up to 3 kA beam current. Since this same design may be used in much longer accelerators our future plans include inserting a "tickler" cavity in the beam line to excite the BBU and measure its gain.

In spite of the care taken in minimizing the voltage stress, we have experienced intermittent surface breakdown across the vacuum side of the insulator. Examination of one cell block, which was removed because of this problem, showed that the breakdown was occurring over the lower part of the insulators, suggesting that it might be due to dust or debris on this surface. If our investigation establishes that this is the cause, then adoption of clean-room techniques during assembly may be necessary to overcome this problem. In the mean time we have derated the allowed gap voltage from its maximum value. This has not kept us from running at 6 MeV in the present operation, but 10 MeV operation will require not only the addition of two more ten-cell blocks but also an increase in the gap voltage from 83 to 112.5 kV.

3.3. Magnetic alignment and beam transport

Initial misalignment of the beam at a small angle with respect to the solenoidal guide field of the accelera-

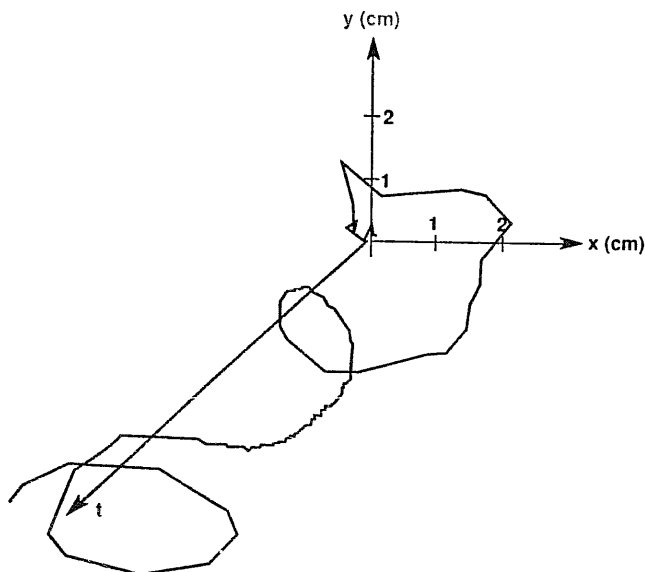


Fig. 4. Example of corkscrew motion of the beam centroid at the exit of the accelerator as a function of time during the time interval that the beam current exceeds one half its maximum value.

tor will result in the beam centroid following a helical path whose phase angle with respect to the injection value is $2\pi f(dz/\lambda_c)$, where $\lambda_c = qB/\gamma m$. Localized field errors with components perpendicular to the beam path will introduce jumps in the guiding-center radius and position along the way. Nevertheless, if the energy is constant, the orbit will be fixed in space, i.e. the X , Y intercept of the beam centroid with a plane normal to the Z -axis for any value of Z will be fixed in time. Energy variation of the beam will result in a variation of the cyclotron wavelength and consequently a complicated sweeping in time of the centroid X , Y location and angle at any position along the accelerator axis. This behavior, which is descriptively called corkscrewing can play havoc with beam transport and imposes stringent requirements on magnetic alignment with the mechanical axis. Specifically, for efficient FEL operation the sweep amplitude at the wiggler entrance should be less than 1 mm. Production of a magnetic axis straight to within 0.1 mm and alignment of the beam with it is necessary to meet this requirement.

The cells are assembled into ten-cell units or blocks. To facilitate the magnetic alignment, a set of sin/cos correction coils was wound on each solenoidal magnet of the induction cells. The ratios of correction coil current to solenoid magnet current necessary to produce a relatively straight (~ 0.1 mm) magnetic axis were obtained by mapping a low-energy electron beam through the individual cell blocks [8].

During the assembly of the accelerator, the injector and six ten-cell blocks were aligned on rails using standard surveying techniques. Between the cell blocks there are at least two intercell solenoids which at present can only be mechanically aligned. Field errors in these magnets appear to be the source of misalignment which combined with the energy sweep has led to an excessive amount of corkscrew behavior. This is illustrated in fig. 4 where the movement of the beam centroid at the exit of the accelerator is plotted as a function of time during a period when the current exceeded half its maximum value. This behavior is observed using resistive-foil wall-return-current monitors [9] ("beam bugs") to measure the beam current and X , Y location of the centroid in the plane of the beam bug. Fig. 5 shows measurements taken in the transport region between the accelerator and the wiggler over a time period when the beam energy varied by approximately $\pm 2\%$ (time between points is ~ 0.8 ns). This data from a pair of beam bugs separated by a field-free region was used as input into the beam transport code to calculate the variation in (x, x') and (y, y') at the wiggler entrance. The output was then used in the FRED [10] code to estimate the effect on the FEL power. The code predicts about a factor of 2 reduction in power over that expected from a perfectly aligned beam.

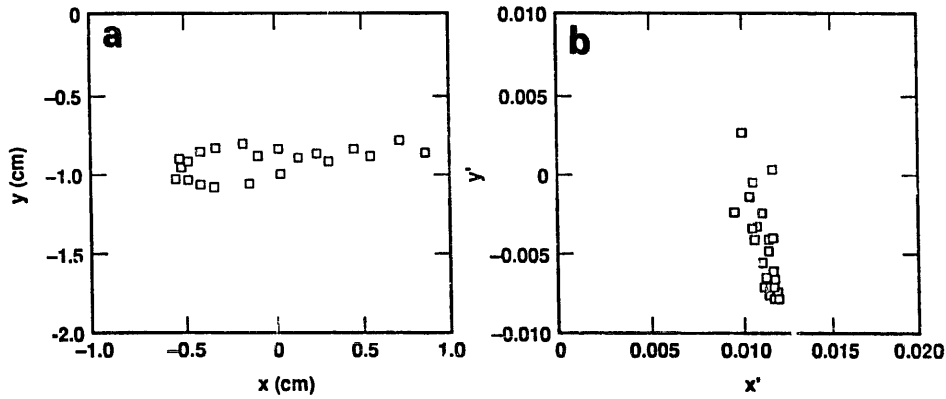


Fig. 5. The centroid position X, Y (a) and angle X', Y' (b) in a field-free section of the transport region between the accelerator and wiggler over a time period when the beam energy varied by $\sim \pm 2\%$ (time between points is ~ 0.8 ns).

3.4. Beam energy variation

A magnet, located in the transport section between the accelerator and wiggler, when energized, deflects the beam into a 45° side arm (fig. 6a). Two pairs of beam bugs, one set on the input side and the other coaxial

with the side arm are used to measure the variation of the deflection angle $\delta\theta$ of the beam centroid in the bending plane around the 45° central angle. The variation in the beam kinetic energy is $dT/T = -(1 + 1/\gamma) \delta\theta$, where T , the energy corresponding to a 45° deflection, is determined from the magnet calibration.

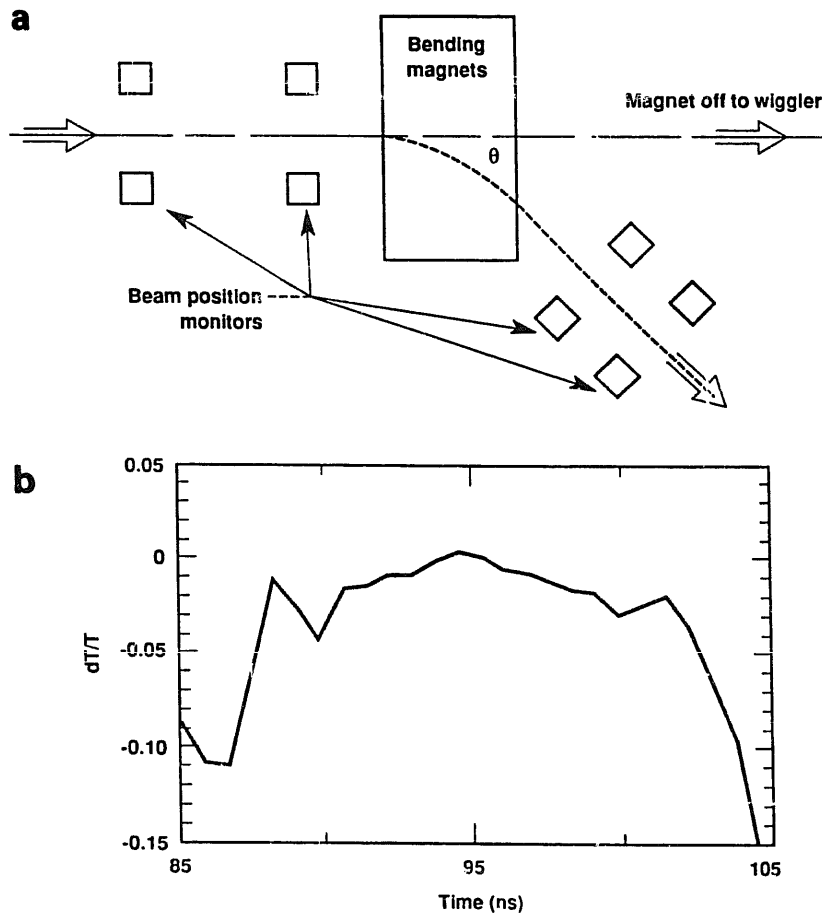


Fig. 6. (a) Schematic of the energy measurement technique. (b) Time variation of the beam energy around its maximum value.

Bit resolution at present limits the measurement of relative energy variations to $\sim 0.1\%$.

Efficient FEL operation requires that beam energy variation be constrained to $\sim \pm 1\%$ around the resonant value. In present operation the observed period during which the energy variation is in the required range has been limited to around 10 ns (fig. 6b). Some small improvement can perhaps be obtained by adjustment of the relative timing between the cell blocks, but extensive modifications to the pulse power hardware (see section 4.3) will be necessary to obtain a flat 50 ns wide pulse.

3.5. Beam brightness

Beam brightness is defined as the beam current density per unit solid angle. We measure it with a field-free, two-aperture collimator similar to that described in detail in ref. [9]. The diagnostic is located in the transport region between the accelerator and wiggler. The two 1.5 mm radius apertures, separated by a distance of 67.5 cm, are mounted on modified gate valves, allowing them to be easily inserted for a measurement or removed to allow transport to the wiggler. Beam bugs located on either side of each aperture measure the current incident upon and transmitted through the aperture. The (normalized) beam brightness is given by $J = I_3 / [(\beta\gamma)^2 V_4 \delta]$ where I_3 is the current through the second aperture, $\beta\gamma$ is the usual relativistic factor, $V_4 = \pi^2 a^4 / L^2 = 1.1 \times 10^{-10} \text{ (m rad)}^2$ and δ is a space-charge correction [12] which is close to unity for our parameters. Initial measurements of the beam brightness have yielded values of about $4 \times 10^8 \text{ A/(m rad)}^2$ at 6 MeV and 1.5 kA. These measurements at present are limited by beam corkscrew which keeps the apertures from being filled except for very short periods of time. The ST code [11] predicts a brightness of $9 \times 10^8 \text{ A/(m rad)}^2$ at the end of the accelerator for the beam from the present injector design.

The microwave FEL experiments require a normalized beam brightness at the wiggler in the range of 3×10^7 to $5 \times 10^8 \text{ A/(m rad)}^2$. Earlier measurements with a triode configuration gave a brightness value of $5 \times 10^9 \text{ A/(m rad)}^2$ at 1.5 kA and 2.7 MeV beam energy [13]. For a high-power microwave FEL the brightness of the diode configuration appears to be adequate and the design has the advantage of being able to provide a beam current of 3 kA at a voltage (1 MV) where breakdown is not a problem.

4. Development

A method for magnetic alignment of the complete accelerator has been developed, and two test stands, important to meeting the ETA-II goal of high average power, are either operating or approaching operation.

4.1. Low-energy electron probe (LEEP)

We have designed and are building a low-energy electron probe (LEEP) diagnostic for magnetically aligning the complete accelerator in situ. It features a two-point feedback-stabilized laser whose beam is aligned parallel to the mechanical axis. A low-energy electron beam ($\approx 4 \text{ keV}$) is injected along the axis from one end and a boat equipped with lateral effect photodiodes (LEPs) and a tilt sensor is pulled the length of the accelerator (fig. 7) while the laser with split parallel beams is launched from the opposite end. The laser beam is split so that one beam is intercepted by an LEP on the boat while the other beam is transmitted to a fixed quad cell at the other end of the machine. Signal from the quad cell is fed back to the pointing mirror controls to maintain a fixed aiming of the two beams. The e-beam transverse position is measured by one of the two LEPs on the boat while the transverse position of the boat is determined by measuring where the laser

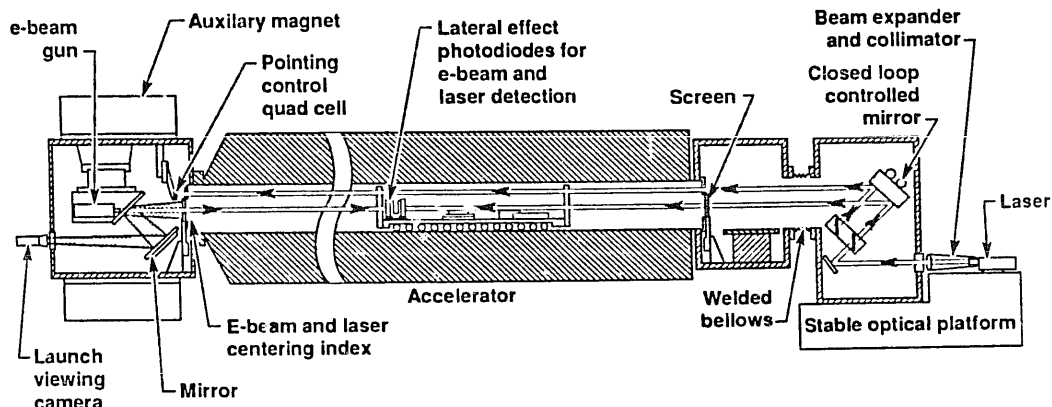


Fig. 7. The low-energy electron probe (LEEP) diagnostic intended to be used for in-situ magnetic alignment of the entire accelerator.

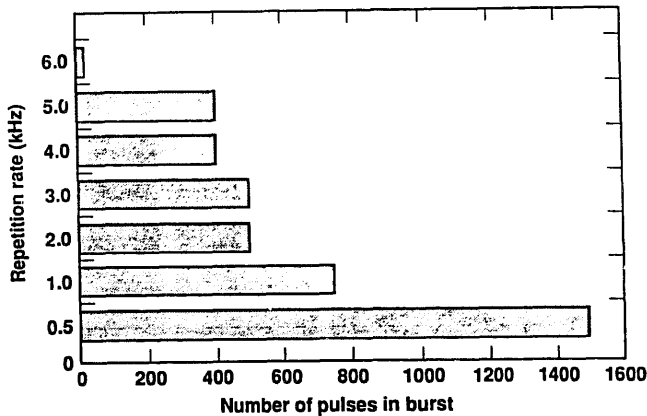


Fig. 8. High-average-power (HAP) test stand results showing the burst length that has been achieved for various PRFs.

strikes the second LEP. True motion of the e-beam and thus of a flux line is determined by subtracting the apparent e-beam position from the boat position, with appropriate consideration for tilt. This technique should allow us to adjust correction-coil current ratios with the necessary accuracy to align the magnetic axis with the mechanical axis within the required 0.1 mm. Without feedback this type of system has been used to align single ten-cell sets to ± 0.1 mm [8]. However, problems with laser pointing stability prevented the satisfactory alignment of the entire accelerator and has led to the feedback-stabilized system illustrated in fig. 7.

4.2. The high-average-power (HAP) test stand

ETA-II as presently configured is limited to a few Hz operation by its primary power supply. A capacitor bank, now under construction, will allow 5 kHz oper-

ation for 10 ms but the long-range goal of 0.5 s pulses will require purchase of new power supplies. In the meantime the HAP test stand, which consists of an ETA-II type pulse power chain supplied with sufficient input power to allow high prf operation, is demonstrating the ability of these units to handle high average power. Fig. 8 shows that 750 ms bursts at 0.5 kHz and 80 ms bursts at 5 kHz have been discharged into resistive loads.

4.3. Multicable feed and passive compensation tests

As presently configured, each cell block of ETA-II is fed from its MAG-1D by a single 4Ω cable. The bus structure distributing the power to the individual cells perturbs the fidelity of the pulse, i.e., the high-voltage pulse waveform varies from cell to cell. In addition, the impedance variation of the cell ferrites during the voltage pulse is not taken into account. As a result the energy regulation goal of $\pm 1\%$ can only be met for a period of about 10 ns and to extend this time to 50 ns will require reconfiguration of the cell block power feed plus passive compensation.

We have designed and will soon be testing a multicable feed design which uses ten solid dielectric 40Ω coaxial cables, five to a side to power each cell block. For symmetry, pairs of cells are supplied in parallel by two cables on opposite sides. The result will be that all cell pairs driven by the same PPU will be fed alike.

The chosen method for passive compensation for the nonlinear load of the accelerator cores and beam current is to taper the pulse-forming line (PFL) in the final stage of the MAG-1D. Normally the PFLs (which are water-filled coaxial transmission lines) are of constant geometry and therefore constant impedance over their

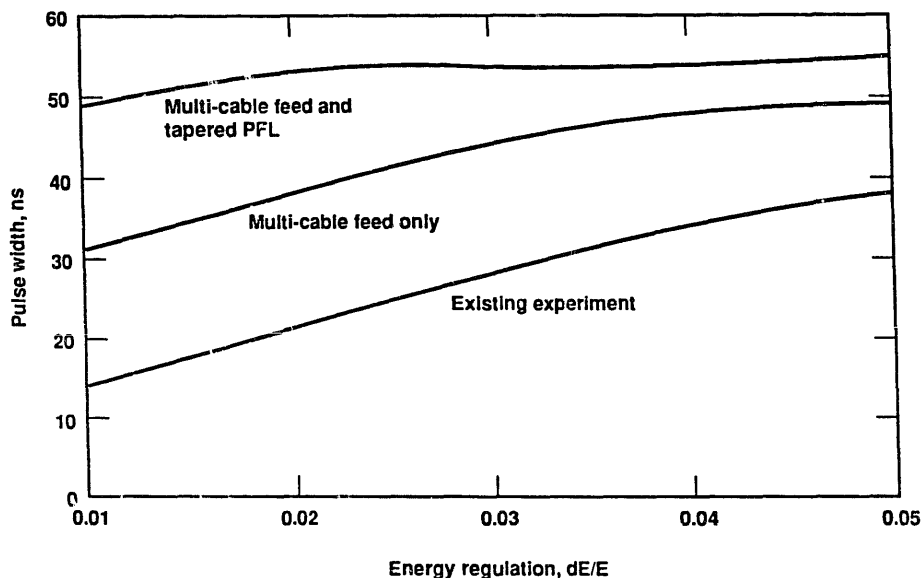


Fig. 9. Results of simulation of ETA-II energy regulation with the multicable feed and tapered PFL.

lengths; however, with a controlled taper of the PFL inner radius we can vary the output voltage to compensate for the beam load and ferrite response. This approach leads to the minimum energy loss compared to other means of compensation such as external networks.

A code model predicts that with the above modifications the energy regulation goal can be met (fig. 9) at the cost of increased sensitivity to beam timing and magnitude of beam current.

5. Summary

As a test bed for high-average-power technology the ETA-II program has met its initial program goals. Magnetic alignment and energy flatness are perceived as the most important problems faced in meeting the future goal of high average power.

Solutions for these problems are ready to be implemented and tested on ETA-II:

- LEEP will be used for magnetically aligning the entire accelerator.
- Replacement of present cell block pulse power feeds with multicable feeds plus tapered PFLs should give the required energy flatness.

References

- [1] D.W. Hewett and J.K. Boyd, *J. Comp. Phys.* 70 (1987) 166.
- [2] W.C. Turner, Y.-J. Chen, W.E. Nexsen, M.C. Green, G. Miriam and A.V. Nordquist, *Proc. 1988 Linear Accelerator Conf.*, Williamsburg, VA, USA, October 2-7, 1988, CEBAF Report 89-001 (June 1989) p. 341.
- [3] R.J. Briggs, D.L. Bix, G.J. Caporaso, V.K. Neil and T.C. Genoni, *Particle Accelerators* 18 (1985) 41.
- [4] D. Bix, L. Reginato, D. Rogers and D. Trimble, LLNL report UCRL-95317 (1986).
- [5] S.J. Sackett, *Users Manual*, LLNL Report UCID-17814 (June 23, 1978).
- [6] W.C. Turner, G.L. Caporaso, G.D. Craig, J.F. DeFord, L.L. Reginato, S. Sampayan, R.W. Kuenning and I.D. Smith, *Proc. BEAMS'88, 7th Int Conf. on High-Power Particle Beams*, Karlsruhe, FRG, July 4-8, 1988 (Kernforschungszentrum Karlsruhe GmbH, II, 1988) p. 845.
- [7] W.E. Nexsen and W.C. Turner, *J. Appl. Phys.* 68 (1990) 298.
- [8] J.C. Clark, F.J. Deadrick, J.S. Kallman, S.S. Tien and W.C. Turner, LLNL report UCRL-99593 (1989).
- [9] K.W. Struve, *Measurement of Electrical Quantities in Pulse Power Systems - II* (National Bureau of Standards, Gaithersburg, MD, 1986).
- [10] R.A. Jong, W.M. Fawley and E.T. Scharlemann, in: *Modeling and Simulation of Laser Systems*, ed. D.L. Bullock, *Proc. SPIE* 1045 (1989) 18.
- [11] J.K. Boyd, W.B. Colson and E.T. Scharlemann, *Proc. 9th Int. Free Electron Laser Conf.* Williamsburg, VA, USA, 1987, *Nucl. Instr. and Meth. A*272 (1988) 590.
- [12] G.J. Caporaso, LLNL Report UCID-20527 (1985).
- [13] W.C. Turner, J.K. Boyd, J.C. Clark and W.E. Nexsen, *Proc. 1989 IEEE Particle Accelerator Conf.*, Chicago, 1989, vol. 2, IEEE Catalog no. 89CH2669 (1989) p. 996.